7th Canadian Conference on Earthquake Engineering / Montreal / 1995
7ième Conférence canadienne sur le génie paraséismique / Montréal / 1995

Seismic Response of Flexible Rotating Machines

W.-C. Su[1] and A.G. Hernried[2]

ABSTRACT

Flexible rotating machine are significantly complex, even for highly simplified models, due to gyroscopic and other effects. This paper presents the coupled, linear partial differential equations of motion of a flexible rotating shaft subjected to ground motion. Classical and finite element methods are developed to solve these equations. The effects of various physical parameters on the response of the system; magnitude, duration, and frequency content of the ground motion; bearing stiffness and damping; flexibility of the shaft; angular velocity of the shaft; as well as forward and reverse rotation are investigated. Both vertical and horizontal ground motions, individually and in combination, will be considered.

A NEWTONIAN APPROACH FOR DETERMINING THE EQUATIONS OF MOTION FOR A ROTATING FLEXIBLE SHAFT

The differential equations for the rotor will be derived by the theory of classical dynamics[1]. The rotor model takes into account bending deformations, rotatory inertia as well as gyroscopic effects. The shaft is assumed rigid in the direction of the axis of the shaft and shear deformations are neglected.

For a uniform symmetric shaft, let $\mathbf{e}_x$, $\mathbf{e}_y$ and $\mathbf{e}_z$ be mutually perpendicular unit vectors fixed in inertia reference frame. Let $\mathbf{e}_q$, $\mathbf{e}_r$ and $\mathbf{e}_s$ be a set of mutually perpendicular unit vectors fixed to a differential element B with symmetric and circular cross section rotating in the inertial reference frame N as shown in Figure 1. The shaft is modelled as a Euler-Bernoulli beam. Let G be the mass center of B, and P be a typical particle in B as shown in Figure 1. Then the acceleration of P and G in the inertial reference frame N, ${}^N\mathbf{a}^P$ and ${}^N\mathbf{a}^G$, are related by the expression[1]

$$ {}^N\mathbf{a}^P = {}^N\mathbf{a}^G + {}^N\alpha^B \times \mathbf{r} + {}^N\omega^B \times ({}^N\omega^B \times \mathbf{r}) \tag{1} $$

where ${}^N\omega^B$ and ${}^N\alpha^B$ are the angular velocity and angular acceleration of differential element B in the inertial reference frame N and can be expressed as[1]

$$ {}^N\omega^B = \Omega_q \mathbf{e}_q + \Omega_r \mathbf{e}_r \; ; \; {}^N\alpha^B = \dot{\Omega}_q \mathbf{e}_q + \dot{\Omega}_r \mathbf{e}_r \tag{2} $$

The equivalent inertia torque $\mathbf{M}^*$ is defined as

$$ \mathbf{M}^* = -\int_B \mathbf{r} \times {}^N\mathbf{a}^P \, dm \tag{3} $$

where dm is a differential mass located at P. By substituting equation (1) into equation (3), the inertia torque $\mathbf{M}^*$ becomes

$$ \mathbf{M}^* = -\int_B \mathbf{r} \times {}^N\mathbf{a}^G \, dm - \int_B \mathbf{r} \times ({}^N\alpha^B \times \mathbf{r}) \, dm - \int_B \mathbf{r} \times [{}^N\omega^B \times ({}^N\omega^B \times \mathbf{r})] \, dm \tag{4} $$

[1] Graduate Research Assistant, Dept. of Civil Engineering, Corvallis, OR 97331.
[II] Associate Professor, Dept. of Civil Engineering, Corvallis, OR 97331.

If G is the mass center of B, the sum of the first mass moments relative to G is zero. After some manipulations[4], the inertia torque $\mathbf{M}^*$ in equation (4) can be rewritten as

$$\begin{aligned} M^* &= -\int_B r\times({}^N\alpha^B\times r)dm - {}^N\omega^B\times\int_B r\times({}^N\omega^B\times r)dm \\ &= -I^{B/G}\,{}^N\alpha^B - {}^N\omega^B\times(I^{B/G}\,{}^N\omega^B) \end{aligned} \tag{5}$$

where $\mathbf{I}^{B/G}$ is the inertia matrix of the differential element B relative to the mass center G for mutually perpendicular unit vectors $\mathbf{e}_q$, $\mathbf{e}_r$ and $\mathbf{e}_s$, i.e.

$$I^{B/G} = Diag[I,\ I,\ J] \tag{6}$$

where the mass moment and polar mass moment of an element of the shaft per unit length can be expressed as $I=\rho Ak^2$ and $J=2\rho Ak^2$ and ρ, A and $k^2(=I/A)$ are the mass density, cross sectional area of the shaft and the radius of gyration of the cross section, respectively.

The components of ${}^N\omega^B$ parallel and perpendicular to ${}^N\omega^B$ are expressed as

$${}^N\omega^B = (e_s\cdot{}^N\omega^B)e_s+(e_s\times{}^N\omega^B)\times e_s \tag{7}$$

Combining equation (7) with equation (6), we have

$$I^{B/G}\,{}^N\omega^B = Je_s\cdot{}^N\omega^B e_s+I(e_s\times{}^N\omega^B)\times e_s \tag{8}$$

Taking the cross product between ${}^N\omega^B$ and both sides of equation (8), substituting the result into equation (5) and using equation (2), the inertia torque $\mathbf{M}^*$ becomes

$$M^* = -(I\dot{\Omega}_q-J\Omega_s\Omega_r)e_q-(I\dot{\Omega}_r+J\Omega_s\Omega_q)e_r \tag{9}$$

The moment acting on the element is (see Figure 2)

$$M=[M_x(z+dz)-M_x(z)-V_y(z)dz]e_q+[M_y(z+dz)-M_y(z)-V_x(z)dz]e_r \tag{10}$$

The shaft is assumed to be a Bernoulli-Euler beam i.e. $M_x=-EIv''$ and $M_y=EIu''$. Considering d'Alembert's principle $\mathbf{M}^*+\mathbf{M}=\mathbf{0}$ and combining equations (9) and (10) with the kinematic relations, $\Omega_r=u'$, $\Omega_q=-v'$, results in

$$\frac{\partial^2}{\partial z^2}\left[EI\frac{\partial^2 u}{\partial z^2}\right] - \frac{\partial^2}{\partial z^2}\left[mk^2\left(\frac{\partial^2 u}{\partial t^2}-2\Omega_s\frac{\partial v}{\partial t}\right)\right] + m\frac{\partial^2 u}{\partial t^2} = 0 \tag{11}$$

$$\frac{\partial^2}{\partial z^2}\left[EI\frac{\partial^2 v}{\partial z^2}\right] - \frac{\partial^2}{\partial z^2}\left[mk^2\left(\frac{\partial^2 v}{\partial t^2}+2\Omega_s\frac{\partial u}{\partial t}\right)\right] + m\frac{\partial^2 v}{\partial t^2} = 0 \tag{12}$$

where m is mass per unit length. For a uniform shaft without disk, the coupled equations for the bending of a rotating shaft for in two directions are given by equations (11) and (12). These two equations of motion can be combining by introducing the symbol $q=v+iu$, resulting in one complex equation, i.e.

$$\frac{\partial^2}{\partial z^2}[EI\frac{\partial^2 q}{\partial z^2}]-\frac{\partial^2}{\partial z^2}[mk^2(\frac{\partial^2 q}{\partial t^2}-2\Omega i\frac{\partial q}{\partial t})]+m\frac{\partial^2 q}{\partial t^2}=0 \tag{13}$$

For a uniform rotor-pin model shown in Figure 3, the eigenfunctions[2] of the above complex equation are

$$q(x,t)=C\sin(\frac{n\pi x}{L})e^{i\lambda t} \quad (n=1,2,3....) \tag{14}$$

where the unknown constant C depends upon the initial conditions. The length of the shaft is L and the eigenvalue of the shaft is λ. For other boundary conditions, the eigenfunctions are provided by Genta[2]. Substitution of equation (14) into equation (13), gives the algebraic equation for the natural frequencies, i.e.

$$(1+\frac{k^2n^2\pi^2}{L^2})\lambda^2-2\Omega\frac{k^2n^2\pi^2}{L^2}\lambda-\frac{EI}{m}\frac{n^4\pi^4}{L^4}=0 \tag{15}$$

Solving equation (15) for a natural frequency λ, results in

$$\lambda=(\frac{k^2n^2\pi^2}{L^2})\frac{\Omega\pm\sqrt{\Omega^2+(1+\frac{k^2n^2\pi^2}{L^2})\frac{EI}{mk^2}}}{1+(\frac{k^2n^2\pi^2}{L^2})} \tag{16}$$

Equation (16) yields two values for λ, one positive and the other negative. In equation (15), forward rotation is given by a positive value for Ω while reverse rotation is given by a negative value for Ω.

In particular, the forward critical speeds Ω_{cf} and reverse critical speeds Ω_{cr} can be obtained by substituting $\lambda=\Omega$ and $\lambda=-\Omega$ into equation (15), resulting in

$$\Omega_{cf}=\frac{n^2\pi^2}{L^2}\frac{\sqrt{\frac{EI}{m}}}{\sqrt{1-\frac{k^2n^2\pi^2}{L^2}}} \; ; \; \Omega_{cr}=\frac{n^2\pi^2}{L^2}\frac{\sqrt{\frac{EI}{m}}}{\sqrt{1+\frac{3k^2n^2\pi^2}{L^2}}} \tag{17}$$

For a particular value of n, the natural frequency λ can be determined as a function of Ω, resulting in a family of curves (see Figure 6). In this figure, the critical speeds of forward and reverse rotation are easily determined by the intersection of the individual curves with the lines $\lambda=\Omega$ and $\lambda=-\Omega$.

FINITE ELEMENT EQUATIONS FOR THE ROTATING FLEXIBLE SHAFT

Finite Element Equations for the Shaft

Finite element formulations have been provided several authors[3,4]. The formulations presented here follow Suarez et. al.[3] closely. The element equations[4] considering translational base motions only and neglecting shear deformations and rotatory inertia are

$$\boldsymbol{M}^e\ddot{\boldsymbol{q}}^e + \boldsymbol{C}^e\dot{\boldsymbol{q}}^e + \boldsymbol{K}^e\boldsymbol{q}^e = \boldsymbol{f}^e(t) \tag{18}$$

where the element mass, damping, stiffness and applied force matrices are defined as

$$M^e=\int_0^l \rho AN^TNds+\int_0^l \rho I_x N'^T N'ds \tag{19}$$

$$C^e=\Omega\int_0^l I_p N'^T(e_1e_2^T-e_2e_1^T)N'ds \tag{20}$$

$$K^e=\int_0^l EI_x N''^T N''ds \tag{21}$$

$$f^e(t)=-\int_0^l [\rho AN^Tds]a_b \tag{22}$$

where $\mathbf{e}_1(=[1, 0]^T)$ and $\mathbf{e}_2(=[0, 1]^T)$. Note that gyroscopic effects are included as evidenced by the term C^e in equation (20). The mass density of the shaft and the vector of translational base accelerations are ρ and $\mathbf{a}_b$, respectively. The shaft transverse and polar mass moment of inertia are I_x and I_p, respectively.

In order to satisfy continuity requirements, the interpolation functions must be continuous in displacement and slope across the element boundaries, i.e. C' continuity. The cubic beam polynomials satisfy C' continuity and are an appropriate choice for the interpolation function **N**. For each element, there are two translational degrees of freedom (u_x^e, u_y^e) and two rotational degrees of freedom (θ_x^e, θ_y^e) in the x- and y-directions; therefore, $\mathbf{q}^e$ in equation (18) is an 8×1 vector of nodal displacements and rotations, given by

$$q^e=[u_{x1}^e,\ u_{y1}^e,\ \theta_{x1}^e,\ \theta_{y1}^e,\ u_{x2}^e,\ u_{y2}^e,\ \theta_{x2}^e,\ \theta_{y2}^e]^T \tag{23}$$

where the second subscripts 1 and 2 indicate the nodal displacements of the left and right ends of the element, respectively.

The effects of the shear deformations cannot be neglected when the shaft is short and stocky. The consistent interpolation element (CIE) and reduced integration element (RIE) have been developed by Reddy[5] when shear deformations are considered. An apparently simple and accurate formulation to modify the stiffness matrix of equation (21) to include shear deformation effects using the method of superposition has been suggested by Su[4].

Journal-Fluid-Bearing System

The bearing system (see Figure 4) is often a major source of stiffness as well as damping for the rotating machine and as such significantly affects the dynamic properties of the system. The bearing affects the critical speeds and the stability of the rotor. Fluid-film bearings are generally modelled by two linear orthogonal elastic and damping forces[6] which depend on the displacements and velocities at the bearing location, respectively. The fluid-film reaction force is a function of the speed of rotation, journal length, journal diameter, radial clearance, lubricant viscosity and the weight of the bearing[7].

PARAMETRIC STUDIES

Natural Frequency and Stability Analysis

The complex eigenvalues problem associated with the rotor-bearing system is

$$(M\lambda^2+C\lambda+K)\cdot x=0 \tag{24}$$

where λ is an eigenvalue of the system and $\mathbf{x}$ is the corresponding eigenvector. This complex eigenvalue problem can be solved by introducing an additional unknown eigenvector $\mathbf{y}$, resulting in the 2N×2N eigensystem (N is the number of degrees of freedom),

$$\begin{bmatrix} \mathbf{0} & I \\ -M^{-1}\cdot K & -M^{-1}\cdot C \end{bmatrix} \begin{bmatrix} x \\ y \end{bmatrix} = \lambda \begin{bmatrix} x \\ y \end{bmatrix} \tag{25}$$

where **M**, **C** and **K** are the mass, damping and stiffness matrices of the rotating machine system, respectively. The natural frequencies (ω) and modal damping ratios (β) of the system are

$$\omega = |\lambda| \; ; \; \beta = -\frac{\Re(\lambda)}{\omega} \tag{26}$$

where the magnitude and the real part of a complex number are denoted $|\cdot|$ and $\Re(\cdot)$, respectively. If the motion of a rotor is stable, the real parts of all the eigenvalues (modal damping ratios) must be negative. To obtain the speed at which a rotor would become unstable, one can plot the largest real part of the system eigenvalues against the speed of rotation shown in Figure 7. For the rotor-disk-bearing model, one can observe a change from a negative to a positive value at the critical rotation speeds of about 2310 and 104 rpm.

Parametric Studies

In general, the equations of motion of a rotor-bearing system subjected to seismic excitation are quite complex. It is difficult to integrate these equations analytically; therefore, a step-by-step approach such as the Newmark-β integration scheme is used.

As an example for seismic analysis, consider the rotor-disk-bearing model is shown in Figure 4 whose physical properties are provided in Table 1. The rotor is modelled using 14 finite elements with a total of 60 degrees of freedom. The bearings have stiffness and damping coefficients as given by Earles et al[7] for elliptical bearings with L/D=1. The maximum seismic response of a rotating machine subjected to different components of the El Centro (1940) earthquake and various speeds of rotation are given in Tables 2 and 3 while the response time histories are shown in Figure 8. Note that the rigid body motion induced by the bearing system must be considered when obtaining the actual deformation response of the shaft.

Consider the rotor-disk-pin model shown in Figure 5. The physical properties of the rotor are the same as the rotor-disk-bearing model, expect that flexible bearing supports are replaced with rigid "pin" supports. Damping provided by the bearings that was present in the previous system is absent here, since there is no material damping of the shaft and no damping in the supports. As expected, the response time histories of the disk will not decay with time (Figure 9). The maximum deformation of rotor-disk-pin model subjected to various components of El Centro (1940) earthquake is given in Table 3 for both forward and reverse rotations. Referring to equation (20), the term Ω is replaced with $-\Omega$ for the rotating shaft operating in reverse direction. Only slight differences are observed in the response.

The effects of the shaft flexibility on the natural frequency and critical speed for the rotor-disk-pin model (Figure 3) are given in Figure 10 and Tables 4 and 5. From Figure 10 and comparing Tables 4 and 5, one can readily observe that natural frequencies for forward and reverse rotations have significant differences when the shaft becomes flexible. Conversely, the natural frequencies for the forward and reverse rotations have no

significant differences when the shaft becomes more stiff (see Figure 6).

CONCLUSIONS

The equations of motion of a flexible rotating machine with uniform properties along the shaft, operating with constant speed of rotation, mounted on rigid supports at the ends are developed using classical dynamics. These governing equations of motion can be reduced to a single algebra equation to determine the natural frequencies and critical speeds of rotation.

Finite element methods are used to model non-uniform flexible rotors with rigid disks and complex journal fluid bearing support systems. Instabilities of a typical flexible rotating machine are discussed. The response of the rotating machine to several different components of the El Centro (1940) earthquake are presented. The effect of stiffness and damping of the support bearings on the seismic response of the rotating machine is explored. It is noted that the critical speeds for a flexible machine supported on rigid "pin" supports exhibit negligible difference for forward and reverse rotation, but differ significantly when the shaft becomes flexible.

REFERENCES

1. T. R. Kane and D. A. Levinson, *Dynamic : Theory and Application*, McGraw-Hill Inc., New York, 1985.
2. G. Genta, *Vibration of structures and mechanics*, Spring-Verlage, New York, 1993.
3. L. E. Suarez, M. P. Singh and M. S. Rohanimanesh, "Seismic response of rotating machines," *Earthquake eng. struct. dyn* **21**, pp. 21-36, 1992.
4. Wen-Chyi Su, *Dynamic response of flexible rotating machine subjected to ground motion,* Master of Science Thesis, Dept. of Civil Engineering, Oregon State University, Corvallis, OR, 1994.
5. J. N. Reddy, *Finite element method*, McGraw-Hill Inc., New York, 1993.
6. J. S. Rao, *Rotor Dynamics*, Wiley, New Delhi, 1983.
7. L. L. Earles and A.B.Palazzolo, "Hybrid finite element - boundary element simulation of rotating machinery supported on flexible foundation and soil," *Rotating mechinery dynamics vol.* **21**, pp 371-381, 1987.

ACKNOWLEDGEMENTS

The authors are grateful to Professor C. Smith of Oregon State University for his insightful discussions on rotor dynamics. The partial financial support of the US National Science Foundation under Grant No. CMS - 9301464 is greatly appreciated.

Table 1 Properties of the rotating machine

Shaft :	Bearing system :
Modulus of elasticity, E = 2.078×10^{11} N/m^2	Viscosity, μ = 0.14839 N·s/m^2
Mass density, ρ = 7806 kg/m^3	Diameter of journal, D = 0.229 m
Poisson's ratio, ν = 0.3	Length of journal, L = 0.229 m
Revolutions per minute, Ω = 880 rpm	Clearance, C = 3.8×10^{-4}
	Weight on bearing, W =67120 N
Rigid disk :	L/D ratio =1.0
Disk mass, m_d = 5670 kg	
Transverse moment of inertia, I_x = 3550 kg·m^2	
Polar moment of inertia, I_p = 7100 kg·m^2	

Table 2 Maximum absolute acceleration of the rigid disk for rotor-disk-bearing model.

Rotation Speed (rpm)	El Centro (S00E+Vert) (g)	El Centro (S00E) (g)	El Centro (Vert) (g)
150	0.5202	0.4447	0.5319
880	0.4785	0.4602	0.4138
1500	0.4635	0.4326	0.4230
2250	0.8051	0.5560	0.4774

Table 3 Maximum deformation (mm) of the shaft at mid-span for rotor-disk-pin model.

Rotation Speed (rpm)	El Centro (S00E+Vert) (g)	El Centro (S00E) (g)	El Centro (Vert) (g)
150	0.7655	0.5283	0.5244
880	0.7774	0.5221	0.5151
1500	0.8084	0.5189	0.5054
2250	0.8414	0.5172	0.4872
-150	0.7591	0.5283	0.5224
-880	0.7375	0.5222	0.5151
-1500	0.7151	0.5190	0.5054
-2250	0.6781	0.5173	0.4872

Table 4 The first three natural frequencies (Hz) for a uniform "stiff" shaft ($EI= 8.17\times10^{9}$) with rigid "pin" supports.

Rotation speed (rpm)	ω_1	ω_2	ω_3
150	198.102	786.424	1747.68
880	198.492	787.959	1751.05
1500	198.823	789.265	1753.91
2250	199.225	790.848	1757.39
-150	197.942	785.794	1746.29
-880	197.553	784.263	1742.93
-1500	197.224	782.965	1740.08
-2250	196.826	781.398	1736.64

Table 5 The first three natural frequencies (Hz) for a uniform " flexible" shaft ($EI=8.17\times10^{1}$) with rigid "pin" supports.

Rotation speed (rpm)	ω_1	ω_2	ω_3
150	0.71124	2.82077	6.25897
880	1.25144	4.94553	10.9100
1500	1.81508	7.16272	15.7643
2250	2.55221	10.0640	22.1220
-150	0.55133	2.19077	4.87614
-880	0.31334	1.24955	2.79739
-1500	0.21604	0.86276	1.93599
-2250	0.15364	0.61404	1.37960

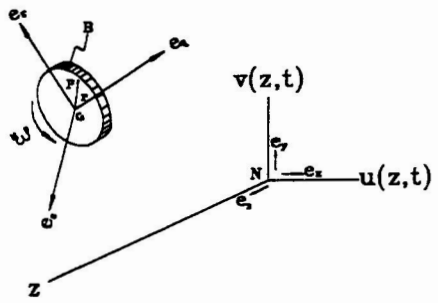

Fig. 1 A differential element B moving in the inertia frame N.

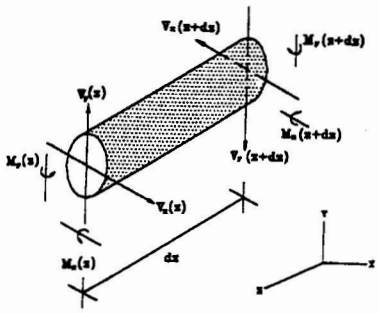

Fig. 2 Free body diagram of the differential element of the shaft.

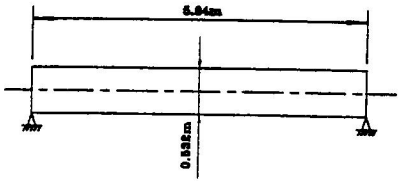

Fig. 3 Rotor-pin model

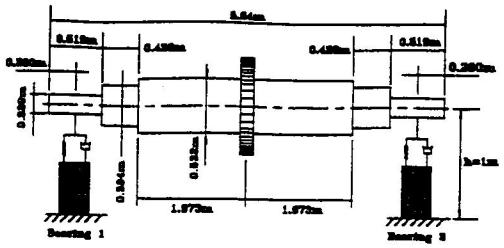

Fig. 4 Rotor-disk-bearing model.

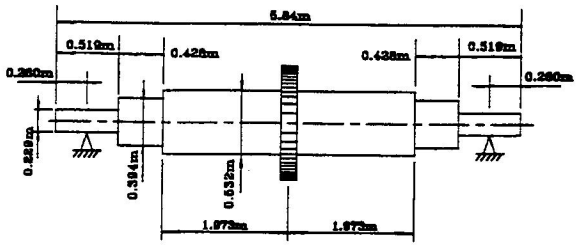

Fig. 5 Rotor-disk-pin model.

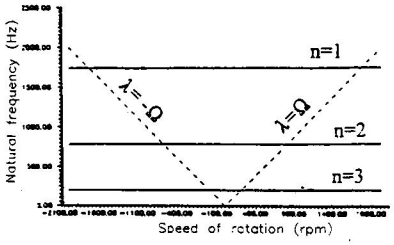

Fig. 6 The natural frequency λ of the stiff shaft with respect to speed of rotation Ωfor a particular value of n.

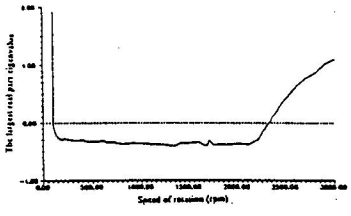

Fig. 7 Variation in the largest real part of the system eigenvalues of the rotor with respect to speed of rotation.

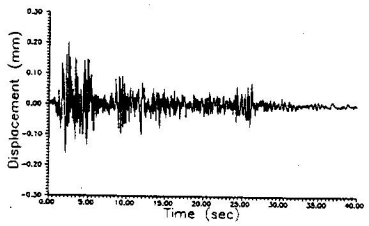

Fig. 8 Time histories of disk displacement in the X-direction for rotor-disk-bearing model with operation speed 880 (rpm) subjected to El Cemtro (1940) earthquake.

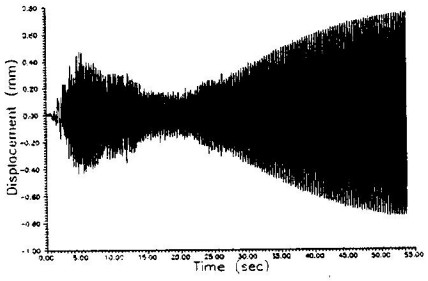

Fig. 9 Time histories of disk displacement in the X-direction for rotor-disk-pin model with operation speed 880 (rpm) subjected to El Centro (1940) earthquake.

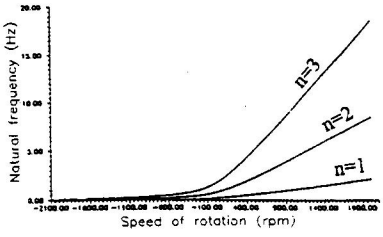

Fig. 10 The natural frequency λ of the flexible shaft with respect to speed of rotation Ωfor a particular value of n.